Investigation of Transformer-Based Solutions for the Reduction of Inrush and Phase-Hop Currents

Rasim Dogan, Saeed Jazebi, *Member, IEEE*, and Francisco de León, *Fellow, IEEE*

***Abstract*—A comprehensive literature review shows that transformer-based solutions are superior for the mitigation of inrush currents than external (to the transformer) solutions. The use of air gaps and low-permeability (iron) materials are known techniques for this purpose. This paper investigates the effectiveness of these approaches for reducing inrush and phase-hop currents. Studies are carried out on toroidal transformers, due to their broad application in power electronics devices. Contrary to common belief, this paper demonstrates that air gaps do not reduce the inrush currents when a transformer is fully demagnetized. However, inrush currents can be mitigated by the use of low-permeability iron materials. It is also demonstrated that air-gaps significantly reduce inrush currents when transformers have residual flux, e.g., for phase-hop conditions. Analytical expressions are derived to compute the mitigation factor for a specific gap length. The results and formulae presented in this paper are verified with laboratory experiments, transient simulations with validated circuit models, and 2-D finite element simulations.**

***Index Terms*—Air-gap, inrush currents, low-permeability materials, phase-hop current, toroidal transformers, UPS.**

I. Introduction

INRUSH currents are usually observed when a transformer core is driven into very deep saturation at the time of energization. The magnitude of inrush currents could be ten to 30 times larger than the rated current depending on the following parameters: switching angle, magnitude and polarity of the voltage, residual flux in the core, saturation inductance of the energized winding, winding resistance, impedance of the source, geometry of the transformer core, and the core material [1], [2].

Transformers can draw more destructive currents compared to inrush currents when the cores have residual flux, or when a phenomenon called "phase-hop" occurs [3]. The magnitude of phase-hop currents might be twice as large as the zero-crossing inrush currents. Phase-hop is not a commonly used term in the literature. However, it needs to be known by power engineers, since a wide range of power electronic devices may create operating conditions which lead a transformer to draw phase-hop currents. Possible reasons for the occurrence of phase-hop current are the switching of uninterruptible power supply (UPS) systems, voltage interruptions, voltage sags, and notching [3].

Manuscript received February 15, 2015; revised June 8, 2015; accepted July 14, 2015. Date of publication July 21, 2015; date of current version December 10, 2015. Recommended for publication by Associate Editor M. Duffy.

The authors are with the Department of Electrical and Computer Engineering, New York University, Brooklyn, NY 11201 USA (e-mail: rd1224@nyu.edu; jazebi@ieee.org; fdeleon@nyu.edu).

Color versions of one or more of the figures in this paper are available online at http://ieeexplore.ieee.org.

Digital Object Identifier 10.1109/TPEL.2015.2459032

Phase-hop and inrush currents are undesirable transient phenomena in power systems. These abnormal events may result in significant voltage drops, which might cause false tripping of protections or produce mechanical stresses on power system components [4]. Thus, power quality, reliability, and stability of the system can be affected.

Several solutions (external to the transformer) have been proposed in the past to mitigate inrush currents. These include: preinsertion resistors [1], negative temperature coefficient thermistors [5], controlled switching [6]–[9], transformer core demagnetization [10], sequential phase energization [11], [12], voltage sag compensators [13], [14], and the application of series dc reactors [15]–[18].

Preinsertion resistors, controlled switching, and core demagnetization need additional control units and detection circuits. Therefore, these circuits reduce the reliability of the system, and increase the complexity and the final cost. Furthermore, they are not applicable for mitigating the phase-hop currents, because of the unpredictability of their occurrence and the lack of time to react even if detected.

Transformer-based solutions, such as reduced flux density designs, air-gaps, use of low permeability (unannealed) iron core, and virtual air-gaps are more robust and effective alternatives [3]. The infallible solution is to design transformers at sufficiently low flux densities so that they never saturate. However, transformers become larger, more expensive, and in some applications there may not be sufficient space to accommodate bulkier transformers. The virtual air-gap technique uses external dc windings on the core [19]. The iron core goes into a local saturation when the dc current is injected. Computer simulation studies in [20] show that the dc excitation creates the same effect as air-gap in the iron core.

It is believed that the use of unannealed cores gives similar performance to the air-gaps with additional advantages [21]. In this paper, the effect of air-gaps and low-permeability iron materials is investigated and the advantages and disadvantages are discussed. Numerous laboratory experiments accompanied with computer simulations indicate that air-gaps are not always capable to mitigate inrush currents especially when a transformer is fully demagnetized.

For the first time, solutions to mitigate the phase-hop currents are presented. It is shown via laboratory measurements that for the inrush cases with initial residual flux and phase-hop, the current amplitude reduces appreciably even with small air-gaps. It is also demonstrated that special designs with low-permeability iron materials could significantly reduce inrush and phase-hop currents. The principal advantage of these methods is their simplicity. These methods do not require any control unit

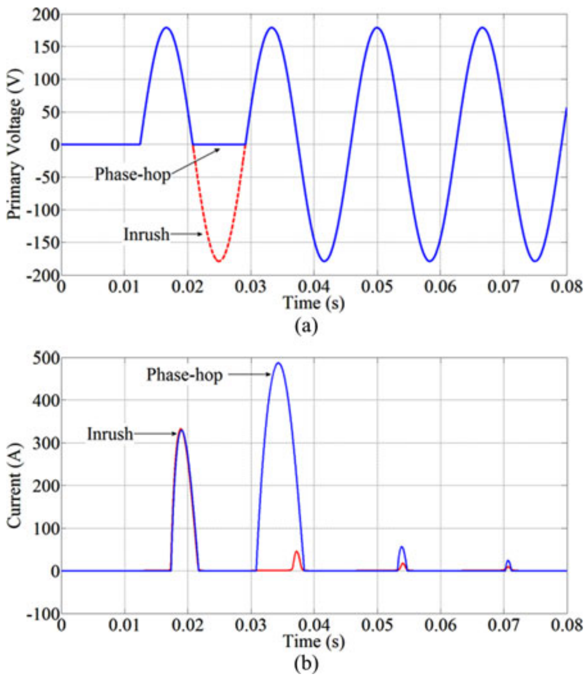

Fig. 1. (a) Transformer primary voltage. (b) Current waveforms during inrush and phase-hop.

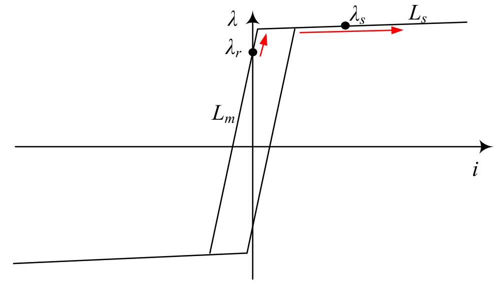

Fig. 2. Hysteresis curve and residual flux.

or monitoring device to detect the phase-hop. Hence, they have perennial functionality.

The phase-hop current is produced by two consecutive semicycles of voltage [see Fig. 1(a)]. The first semicycle builds magnetic flux in the core, which is trapped as residual flux. This causes a higher value of inrush currents when the second semicycle of the voltage is applied to the transformer terminals. The air-gap drains the residual flux and consequently reduces the phase-hop current. Unannealed cores have reduced residual flux when compared to annealed cores. Less residual flux leads to diminished phase-hop currents.

The effectivity of the methods is demonstrated with validated time domain (transient) models using the EMTP-RV and also with finite elements (FEM) simulations using ANSYS Maxwell in 2-D. Transient simulations are performed using the reversible model explained in Section IV. Laboratory experiments are performed on several transformers to corroborate the simulation results and the proposed solutions.

II. Description of Inrush and Phase-Hop Currents

A. Inrush Currents

Inrush currents are transients that occur when transformers are connected to the source. They happen because the magnetic flux is driven by the voltage and the transformer iron core saturates. The peak of this phenomenon is a function of the time of switching, residual flux in the core, resistance and inductance of the system. The worst case happens when the transformer is in open circuit, residual flux is at maximum (see λ_r in Fig. 2), and the switching happens at voltage zero crossing with a polarity that increases the flux in the core.

After the transformer is disconnected from the source, the residual flux depends on the operating point before disconnection. As the result, at the moment of reconnection, the inrush currents may occur at different levels depending on the residual flux. Therefore, in this paper, inrush current experiments are performed on demagnetized transformers to obtain consistent measurements and to be able to validate the transient simulations. A zero-crossing sinusoidal voltage is applied to the transformer on the primary side when the secondary side is open circuit. The primary voltage is illustrated in Fig. 1(a). After a half cycle, the magnitude of the flux in the core is (theoretically) doubled when compared to the maximum flux of the steady-state condition [4]. This high flux drives the core into saturation and inrush currents are drawn from the source.

B. Phase-Hop Currents

Phase-hop currents occur when the transformer goes into supersaturation (more than double of rated flux). Supersaturation is observed when the transformer is energized with a zero-crossing voltage and simultaneously the core has maximum residual flux with the same polarity [3]. This could be explained from the transformer terminal voltage shown in Fig. 1(a). The first half cycle of voltage impresses a high level flux in the magnetic core. Then, the voltage is zero for a half cycle. Therefore, flux remains in the core at the moment the second voltage positive semicycle is applied. Hence, the flux magnitude becomes (theoretically) larger than double. This larger flux drives the core into much deeper saturation when compared with the inrush current condition, and thus, a larger current is drawn from the source [see Fig. 1(b)].

The phase-hop condition is similar in nature to inrush currents with residual flux. However, there are some important differences when comparing the residual flux of phase-hop and inrush conditions. The magnitude of inrush currents depends on the initial conditions, before the zero voltage switching. If the transformer is disconnected from the circuit, then the operating point is on the λ axis at the point of zero current on the magnetizing characteristic; λ_r in Fig. 2. Therefore, the worst case scenario of inrush currents happens with the initial flux of λ_r and at the moment of zero voltage switching, with a polarity of voltage which builds up the flux (in this case positive). On the other hand, phase-hop is a transient that happens when the transformer is magnetized higher than λ_r. For example, in the case of a fault at the primary terminals or when voltage sags happen, the

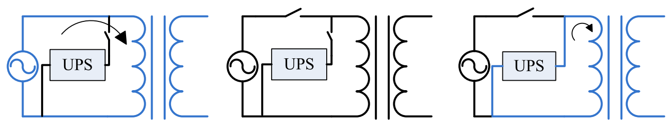

Fig. 3. Phase-hop caused by the normal operation of a UPS system. (a) Normal operating condition. Utility power is on. (b) No power is delivered to the load. (c) Power is supplied by the UPS.

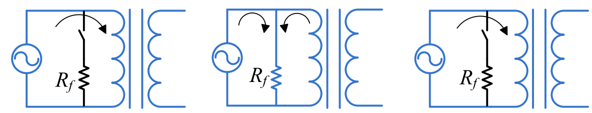

Fig. 4. Phase-hop caused by a short circuit. (a) Normal operating condition. The utility power is on. (b) Short circuit. (c) Short circuit is cleared and power is back.

terminal current will not jump to zero and will keep circulating in the primary winding. Therefore, magnetic flux will be trapped in the core for a period of time that depends on the time constant (total resistance and inductance of the system). The operating point in some cases may stay on the saturated section of the magnetizing curve; for example, λ_s in Fig. 2. In this condition, the worst case scenario also happens at the moment of zero voltage switching with the polarity of voltage which builds up flux. Therefore, phase-hop and the worst case of inrush current (with residual flux) are similar in nature, but the phase-hop condition yields higher currents since the core is at a higher initial flux.

To observe the phase-hop current, two consecutive semicycles of voltage [see Fig. 1(a)] is applied to the transformer on the primary side when the secondary side is open circuited and the transformer is demagnetized. The first half cycle of voltage impresses a high level flux in the magnetic core. The worst case of phase-hop occurs when there is a 0.5 cycle delay between two consecutive voltage semicycles of the same polarity [3]. If there is longer delay than a 0.5 cycle, the residual flux decreases. Therefore, all phase-hop experiments and simulations in this paper are performed based on a half cycle delay to assure the worst possible case.

Several operating conditions of electronic circuits create phase-hop currents. Phase-hop can happen by notching, voltage sags, maloperation of UPS systems, and voltage interruptions in the network. These phenomena can be classified into two main categories:

1) phase-hop caused by a parallel switching action;
2) phase-hop caused by a series switching action.

1) Series Switching: As discussed in [3], the maloperation of offline UPS systems may cause phase-hop currents. This phenomenon happens because of the series disconnection of the UPS system at the terminal of the transformers (see Fig. 3). When the main source is not available, the UPS is switched on to feed the load. The time delay between disconnection of the mains and connection of the UPS may create a phase-hop phenomenon. Therefore, this operation is modeled by series switching.

An interruption is defined as a complete loss of voltage for a specific period of time [22]. This time period could be momentary (from 0.5 to 180 cycles), temporary (from 180 to 3600 cycles), or sustained (more than 3600 cycles) in a 60 Hz system. Possible reasons for interruption are the opening of a line as the result of power system faults, equipment failures, and control systems malfunctions [23]. They all can be represented with a series switching as illustrated in Fig. 3. The only difference between interruption and malfunction of UPS scenarios is that in the interruption the utility power is recovered instead of UPS reconnection.

2) Parallel Switching: Voltage sags are defined as a percentage magnitude value in terms of regular voltage level [23]. They are often the result of faults, typically single line-to-ground fault (SLG), in power systems. Therefore, this phenomenon could be simulated with the switching of a parallel resistance with the terminals of the transformer. This resistance represents the fault impedance (see Fig. 4).

Notching is a disturbance of opposite polarity to the voltage waveform which is frequently caused by malfunctions of the electronic switches or power conditioners [24]. Voltage notching is primarily caused by three-phase rectifiers or converters. Voltage notches happen when the current commutates from one phase to another. Subsequently, a momentary short circuit between two phases will occur during this period [23]. The worst case is when the fault resistance is negligible. Also, it should be noted that this phenomenon last at most for half a cycle. Therefore, notching is a particular situation of the voltage sag case when R_f is equal zero and can be represented with parallel switching as shown in Fig. 4.

TABLE I
INFORMATION OF THE TOROIDAL TRANSFORMERS

Core Dimensions (mm)			Winding Characteristics		
Inner Diameter	Outer Diameter	Height	Primary Turns	Secondary Turns	Wire Gauge
85.7	149.2	50.8	196	196	13

III. Effect of Air-Gap and Low-Permeability Material on the Electromagnetic Behavior of Transformers

In this paper, several toroidal transformers are studied for the mitigation of inrush and phase-hop currents. All transformers are geometrically similar, single-phase, same voltage (120 V), and have 1 kVA rated power. The core dimensions and windings characteristics are shown in Table I. The first prototype (T1) shown in Fig. 5 does not have an air-gap and is wound on an annealed iron core. Prototypes T2 to T7 are wound on annealed iron cores and have 2, 4, 8, 16, 32, and 64 mil total air-gaps ($= 2$ g), respectively. The last transformer (T8) is manufactured on an unannealed core of the same material (M4), thus having a different magnetic permeability than the rest since the manufacturing stresses have not been relieved.

Toroidal transformers have very sharp hysteresis curves when compared to standard transformers because they do not have

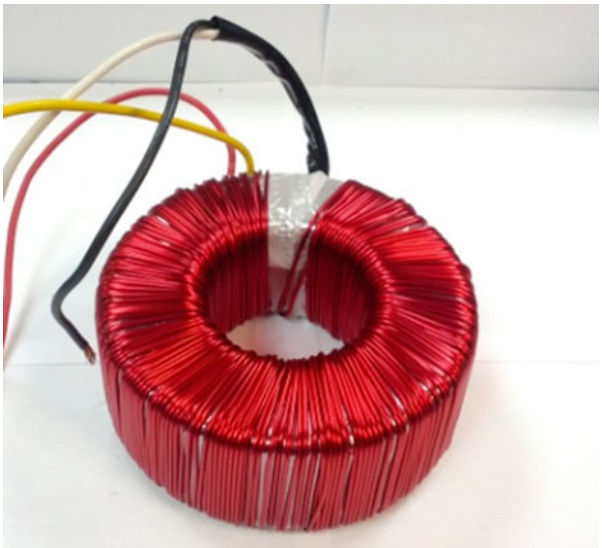

Fig. 5. Toroidal transformer under study (T1).

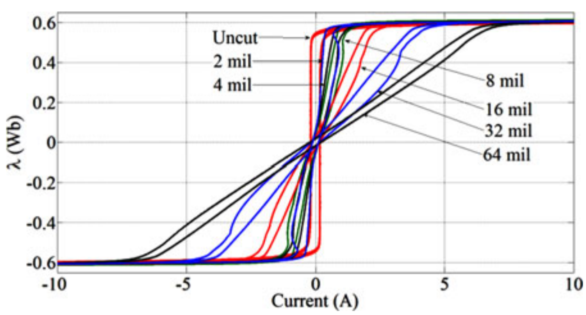

Fig. 6. Hysteresis characteristic of uncut and all gapped transformers obtained by measurements.

air-gaps in the core. The sharp hysteresis curve results in large residual flux because the magnetizing curve crosses at a higher value of flux when the current is zero. The use of air-gaps and low-permeability materials change this characteristic as demonstrated in the following sections.

A. Air-Gap Effect on the Magnetizing Characteristics of Transformers

Open-circuit tests are performed on transformers with different air-gap lengths according to the IEEE Standard C57.12.91-1995 [25]. Hence, the open-circuit tests are performed with 120 V applied to the primary terminal. The primary current and secondary voltage are measured. The linkage flux is derived from the integration of the secondary voltage [26]. As a result, the hysteresis curves for uncut and all six gapped transformers are shown in Fig. 6. The measured residual fluxes (flux corresponding to zero terminal current) for each transformer are presented in Table II (see Fig. 6 as well). Measurements demonstrate dramatic changes in the magnetic behavior of the transformers with different air-gaps lengths. One can observe that the flux follows different magnetizing paths depending on

TABLE II
MEASURED RESIDUAL FLUX FOR TRANSFORMERS

Transformer	$\lambda_{\mathrm{residual}}$ [mWb]
Uncut (T1)	541
2 mil (T2)	57
4 mil (T3)	51
8 mil (T4)	45
16 mil (T5)	28
32 mil (T6)	19
64 mil (T7)	17

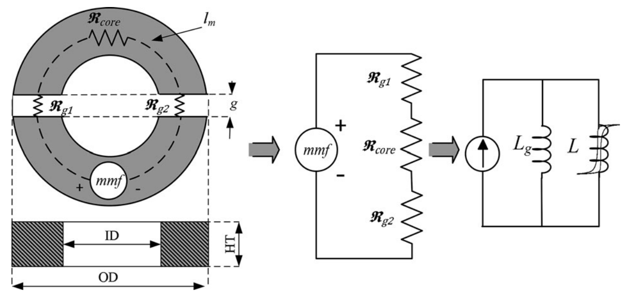

Fig. 7. Dimensions and the magnetic equivalent circuit of the core with air-gap. Note that g is half of the total air-gap. To create air-gaps in the iron core, transformer manufacturers diametrically cut the core into two halves. Then the surfaces are grinded, burnished, and kept apart with Mylar or epoxy fiberglass laminates glued and banded to keep the separation distance well controlled. Finally, the transformer is wound as usual.

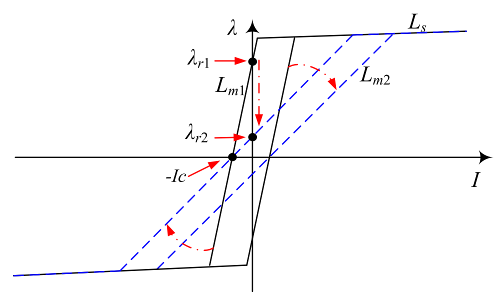

Fig. 8. Hysteresis characteristic (L) of transformer iron core represented by two constant slopes; the effect of the gap (L_g) on the hysteresis curve is shown.

the length of the air-gap. Most importantly, the residual flux reduces noticeably. Therefore, for a transformer with an air-gap, when the terminal current tends to zero at the moment of disconnection from the source, the flux also tends to zero, and the core will be demagnetized.

Theoretically, a larger gap results in a lower slope (see Fig. 6). The reason can be explained from the reluctance circuit of the toroidal transformer shown in Fig. 7 and a piecewise linear approximation of the hysteresis curve (see Fig. 8).

According to the principle of duality between magnetic and equivalent electrical circuits, the air-gap can be represented with a parallel linear inductance with the nonlinear magnetizing branch as shown in Fig. 7 [27]. The parallel connection of the linear inductance (L_g), changes the slope of the magnetizing curve (L) that is shown in Fig. 8. According to this figure, the

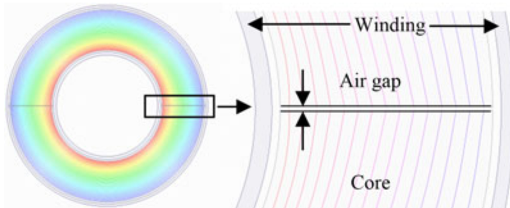

Fig. 9. Magnetic flux lines for a 64 mil gap transformer obtained from 2-D FEM simulations.

following expressions can be written for $\lambda = 0$:

$$0 = L_{m1}(-I_c) + \lambda_{r1} \Rightarrow I_c = \lambda_{r1}/L_{m1} \tag{1}$$

$$0 = L_{m2}(-I_c) + \lambda_{r2} \Rightarrow I_c = \lambda_{r2}/L_{m2} \tag{2}$$

where I_c is the coercive current [28]. Therefore, we get

$$\lambda_{r2} = \frac{L_{m2}}{L_{m1}}\lambda_{r1}. \tag{3}$$

The magnetizing inductance of the transformer with air-gap (L_{m2}) is smaller than the magnetizing inductance of the uncut transformer (L_{m1}). Therefore, the air-gap decreases the residual flux from λ_{r1} to λ_{r2} according to (3). Note from Fig. 7 that, $L_{m2} = L_{m1}||L_g$, hence substituting L_{m2} in (3) yields

$$\lambda_{r2} = \frac{L_g}{L_{m1} + L_g}\lambda_{r1}. \tag{4}$$

Neglecting the fringing effects and assuming a uniform magnetic field (see Fig. 9)

$$\Re_{g1} = \frac{g}{\mu_0 \frac{(OD-ID)}{2} HT} \tag{5}$$

$$\Re_{g1} = \frac{2g}{\mu_0 (OD-ID) HT} \tag{6}$$

$$L_{g1} = L_{g2} = \frac{N^2}{\Re_{g1}} = \frac{N^2 \mu_0 (OD-ID)HT}{2g} \tag{7}$$

where L_{g1} and L_{g2} are the equivalent magnetizing inductances of the air-gap, *N* is the number of turns of the energized winding, *g* is half of the total air gap (i.e., for the 2 mil transformer, $g = 1$ mil), and $\Re_{g1}$ is the reluctance of one of air-gaps. Parameters *HT, ID, OD,* and l_m stand for height, inner diameter, outer diameter, and the mean length of the flux path in the core, respectively (see Fig. 7). Also, μ_0 is the permeability of vacuum $4\pi 10^{-7}\,\mathrm{H/m}$, and μ_r is the relative permeability of the iron core measured as 4000 at the operating voltage (120 V). The inductance of the total air-gap is

$$L_g = L_{g1}||L_{g2} = \frac{L_{g1}}{2} = \frac{N^2 \mu_0 (OD-ID)HT}{4g}. \tag{8}$$

Therefore, we have

$$\lambda_{r2} = \frac{N^2 \mu_0 (OD-ID)HT}{4gL_{m1} + N^2 \mu_0 (OD-ID)HT}\lambda_{r1} \tag{9}$$

where L_{m1} is calculated from the open-circuit test on the uncut core transformer [29] as

$$L_{m1} = \frac{(V_{\mathrm{OC}} - R_s I_{\mathrm{OC}})^2}{2\pi f Q_{\mathrm{OC}}} \tag{10}$$

where V_{OC}, I_{OC} are the rms values of open-circuit voltage and current, Q_{OC} is the open-circuit reactive power and R_s is the resistance of transformer winding. The following formula is used to calculate the maximum inrush current [30]:

$$I_{\max} = \frac{V_m}{\sqrt{(\omega L_s)^2 + R^2}}\left(1 + \cos\theta + \frac{\lambda_r - \lambda_s}{\lambda_n}\right) \tag{11}$$

where V_m is the peak of the voltage, ω is the angular frequency, L_s is the deep saturation inductance, *R* is the total resistance ($R = R_s + R_{\mathrm{sc}}$), θ is the switching angle, R_{sc} is the short-circuit resistance of the system, λ_r is the residual flux, λ_s is the flux at saturation instant, λ_n is the nominal magnetic flux (V_m/ω). Assuming that the hysteresis loss (area of the hysteresis loop) remains the same for the cut and uncut cores and that variations of the saturation flux are negligible ($\lambda_{s1} = \lambda_{s2}$), for the same switching conditions the relative mitigation of phase-hop current is calculated by combining (9)–(11) yielding (12) as shown at the bottom of the page.

Note that the method of [30] includes approximations to derive the simple equation (12) for the calculation of the inrush currents. Our experience shows that this is the most practical formula for the purpose of this study. It is noteworthy to mention that (12) may fail to predict inrush currents especially for transformers with sharp hysteresis curves. We have proposed new analytical methods to compute the maximum inrush and phase-hop currents [31]. This new procedure is based on several formulas and calculation steps, and thus not applicable to the study presented in this paper. Nevertheless, laboratory measurements and simulation studies in this paper show that (12) works accurately enough for the purposes of this paper. The validation of (12) is presented in Section V.

The use of large air-gaps is not practical because the magnetizing current increases and becomes comparable to the nominal current of the transformer. The magnetizing current of the transformers with the air-gap (I_{rms}) could be estimated with the following equations:

$$\Re_{\mathrm{core}} = \frac{\pi(OD+ID)}{\mu_0 \mu_r (OD-ID)HT} \tag{13}$$

$$L_{\mathrm{tot}} = \frac{N^2}{\Re_{\mathrm{gap}} + \Re_{\mathrm{core}}} \tag{14}$$

$$I_{\mathrm{rms}} = \frac{V_{\mathrm{rms}}}{L_{\mathrm{tot}}\omega} \tag{15}$$

$$\mathrm{Mitigation}(\%) = \frac{100(I_{\max 1} - I_{\max 2})}{I_{\max 1}} = \frac{400g(V_{\mathrm{OC}} - R_s I_{\mathrm{OC}})^2 \lambda_{r1}}{[2\pi f Q_{\mathrm{OC}} N^2 \mu_0 (OD-ID)HT + 4g(V_{\mathrm{OC}} - R_s I_{\mathrm{OC}})^2][2\lambda_n + \lambda_{r1} - \lambda_s]} \tag{12}$$

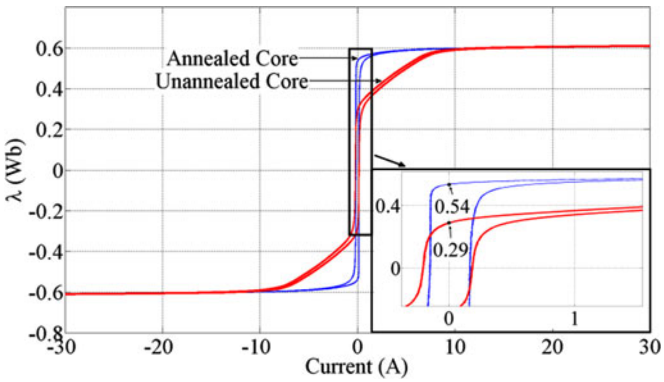

Fig. 10. Annealed (T1) and unannealed (T8) cores hysteresis characteristics, $\lambda = 0.6$ Wb corresponds to B = 1.9 T, $\lambda = 0.54$ Wb corresponds to B = 1.71 T, and $\lambda = 0.29$ Wb corresponds to B = 0.91 T.

where $L_{\rm tot}$ is the total inductance value of the transformer, ω is the fundamental frequency in rad/s, and $V_{\rm rms}$ is the rms voltage of the primary. A comprehensive study on the effect of the gap length and the proper selection of this parameter is carried out below.

B. Unannealed Core Effect on the Magnetizing Characteristics of the Transformers

During core manufacturing, the last step is to anneal the core to fix the molecular structure and reduce the power loss [32]. If the last step is not applied to the core, the iron core has lower permeability and is called an unannealed core. The difference between the magnetizing characteristic of the annealed and unannealed cores is shown in Fig. 10. The unannealed core presents two knees and the annealed core only one.

The unannealed iron core transformer (T8) starts saturating (first knee) at a lower flux density 0.95 T (0.29 Wb) when compared to an annealed iron core transformer (T1) that saturates at 1.77 T (0.54 Wb). The residual fluxes of the two cores are different as well. However, at high saturation, beyond the second knee of the unannealed core, after 1.9 T (0.6 Wb) the two cores behave in the same way. The different magnetic characteristics result in different magnetizing currents and losses in steady state. T8 has a magnetizing current of 1.7 A and 15 W loss, while T1 draws only 0.07 A with 6 W loss. Because of the special behavior of the magnetizing curve of the unannealed iron cores (lower residual flux), transformers built with them draw substantially reduced inrush currents. This can be advantageous if the design calls for a reduced flux density; see the experimental results below.

IV. Transformer Modeling and Parameter Identification

For accurate transient simulations, the reversible π model is selected instead of the traditional T model [26]. Although both T and the reversible π models give the same result during steady state, the reversible π model gives more accurate results in transients involving deep saturation. The reversible model is more accurate and physically meaningful when compared to T model to represent the single-phase transformers. In addition, it is capable to accurately represent transients from both primary and secondary windings.

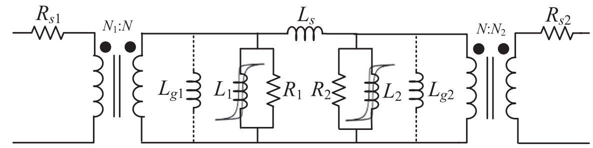

Fig. 11. Reversible π model of transformer including the representation of the air-gap.

The reversible π model can be directly used to represent the unannealed transformer (T8) without air-gap. The only difference between the annealed (T1) and unannealed (T8) transformers in terms of modeling is their different magnetizing characteristics which should be measured from the open-circuit tests and modeled in time domain [25]. However, time domain models for air-gap transformers require modifications.

According to principle of duality (see Fig. 7), for a gap transformer, a linear inductance shall be added in parallel to the magnetizing inductance. Since two nonlinear magnetizing branches exist in the reversible π model, the air-gap inductance L_g is also divided into two linear parts L_{g1} and L_{g2} (see Fig. 11). The value of these inductances can be calculated based on (7). The computed values of L_{g1} and L_{g2} are presented in Table III for all transformers.

To identify other parameters of the model, standard short-circuit and open-circuit tests are performed as per IEEE Standard C57.12.91-1995 [25]. The total series resistance ($R_{s1} + R_{s2}$) of transformers and the leakage inductances (L_s) are obtained from the impedance measurements. The measured ac resistance is broken into primary and secondary sides proportionally to the dc resistances of the windings [26].

The open-circuit test is performed to obtain the transformer magnetizing branch parameters consisting of magnetizing resistances (R_1 and R_2) and nonlinear inductances (L_1 and L_2). The nonlinear inductors correspond to the magnetic behavior of the core. Furthermore, the deep saturation characteristic of the transformer is very important to get precise results during transients drawing very large currents from both windings. Hence, saturation inductance (frequently called the air-core inductance) tests are performed for the transformers according to the guidelines presented in [33]. The geometry of the windings and the number of turns are the same for all transformers; thus, the measured saturation inductances of all transformers are almost identical. In this paper, the small differences between the saturation inductances in different transformers are neglected. The measured value of the saturation inductance is 274 μH. All transformer parameters are presented in Table III. A piece-wise linear approximation of the magnetic characteristics with two slopes is used in the transient simulations (see Table IV).

V. Laboratory Measurements and Validation

To evaluate the effect of the air-gap and low-permeability iron material, experiments are conducted in two stages. First, the effect of the two methods on the ordinary zero-crossing

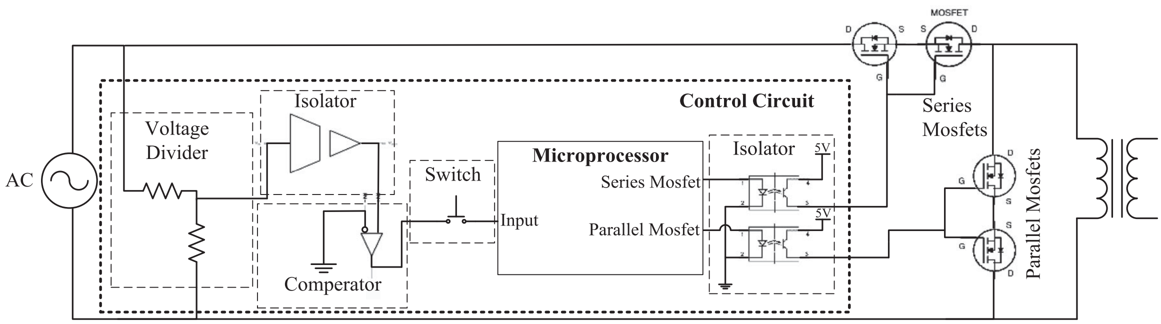

Fig. 12. Circuit diagram of switches.

TABLE III
TRANSFORMER PARAMETERS MEASURED AS PER IEEE STANDARD C57.12.91 EXCEPT THE LAST COLUMN THAT ARE CALCULATED WITH (7)

Transformer	R_{s1} [mΩ]	R_{s2} [mΩ]	L_S [μH]	R_1 [Ω]	R_2 [Ω]	$L_{g1} = L_{g2}$ [mH]
Uncut (T1)	257	271	305	3400	3400	-
2 mil (T2)	251	266	270	3262	3262	3064
4 mil (T3)	255	270	270	3220	3220	1532
8 mil (T4)	252	272	224	3192	3192	766
16 mil (T5)	250	265	260	2880	2880	383
32 mil (T6)	255	267	262	1904	1904	191
64 mil (T7)	252	275	258	1278	1278	95
Unannealed (T8)	260	273	259	1921	1921	-

TABLE IV
NONLINEAR INDUCTANCE CURVE FOR TRANSIENT SIMULATIONS OF ANNEALED CORE

Current [A]	λ [Wb]
−160	−0.71
−0.004	−0.6
0	0
0.004	0.6
160	0.71

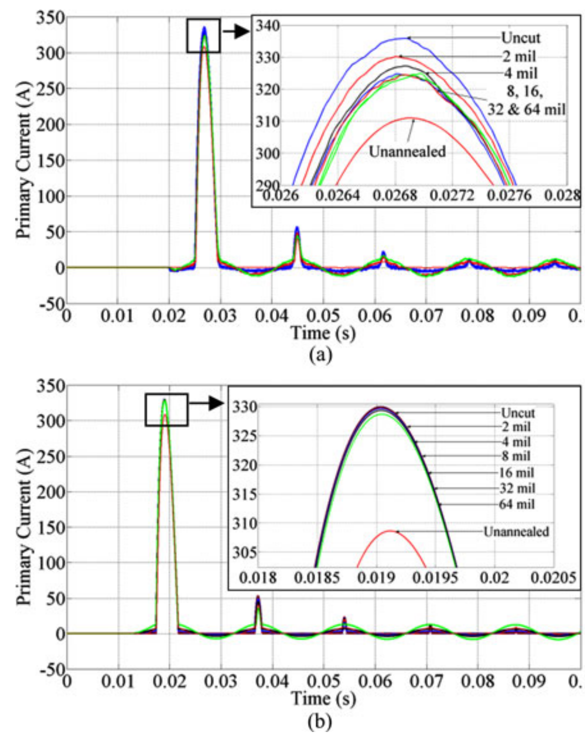

Fig. 13. Inrush currents of all transformers. (a) Measurements. (b) Transient simulations (EMTP-RV).

inrush currents is tested and then the mitigation of the phase-hop current phenomenon is investigated.

A. Inrush Current Experiments

A programmable microcontroller switch is designed to emulate the inrush current conditions described in Section II. This switch consists of two parallel and two series MOSFETs with the terminal of the transformer and a control unit as shown in Fig. 12. Note that the core is completely demagnetized before each experiment. The measurement results for the all transformers are shown in Fig. 13(a). The peak values of the zero-crossing inrush currents are between 325 and 335 A. The results demonstrate that the air-gap has no significant effect on the zero-crossing inrush currents when the core is demagnetized. This is so because the dominant effective factors on the inrush current peak value are the saturation inductance and the terminal resistance [26]. Furthermore, the same transformers are analyzed with transient simulations (EMTP-RV) to validate the π model. These simulations are shown in Fig. 13(b). Almost exactly the same results are obtained with simulations (inrush currents between 328 and 330 A). The peaks of the inrush current for T1, T2, T7, and T8 are shown in Table V.

B. Phase-Hop Current Experiments

As discussed in Section II, there are two general conditions that cause phase-hop currents: series switching and parallel switching. These conditions are emulated with the power electronic device presented in Fig. 12.

1) Voltage Interruption and UPS System Cases: To create the voltage interruption and UPS system disconnection cases in laboratory, the parallel MOSFET of the switch needs to be

TABLE V
EXPERIMENTAL RESULTS VERSUS TRANSIENT AND FEM SIMULATIONS FOR THE INRUSH CURRENT

	Measurement [A]	Transient Simulation [A]	Difference (%)	FEM [A]	Difference (%)
T1	336	330	1.8	330	1.7
T2	330	330	0	330	0
T7	325	329	1.1	328	0.9
T8	310	308	0.6	289.5	6.6

TABLE VI
EXPERIMENTAL RESULTS VERSUS TRANSIENT AND FEM SIMULATIONS FOR THE SERIES SWITCHING TRANSIENTS - PHASE-HOP CURRENT

	Measurement [A]	Transient Simulation [A]	Difference (%)	FEM [A]	Difference (%)
T1	490	484.0	1.22	480.0	2.0
T2	330	329.8	0.06	325.6	1.4
T7	330	330.0	0	328.2	0.5

deactivated. Hence, only the series MOSFET opens and closes when the controller sends the command.

The first set of experiments is carried out on the air-gapped transformers. In this section, only three transformers (T1, T2, and T7) are tested under the phase-hop condition for the series transient cases. All of the three transformers are demagnetized before phase-hop tests. Therefore, the result is not affected by the residual flux. The laboratory test setup is also implemented in transient and FEM simulations. The peaks of the phase-hop current for these three transformers are shown in Table VI. The results of simulations and measurements are compared for T1 and T2 in Figs. 14 and 15. In these figures, the first peak of the current reflects the zero crossing inrush current for the demagnetized transformer. The second peak is the phase-hop condition. These results show that the phase-hop current magnitude is reduced by even a small air-gap (T2) to the zero crossing inrush current magnitude with zero residual flux. Also, the excellent agreement between the simulations and experiments demonstrates the validity of the simulations.

The effect of the air-gap is clearly seen with the comparison of Figs. 14 and 15. The voltage waveforms for T2 (see Fig. 15) are different from T1 (see Fig. 14). The significant difference in the voltage waveform of Figs. 14 and 15 is the high negative peak seen in Fig. 15. This means that the linkage flux is reduced in the cut transformer when the switch is open. Therefore, the air-gap transformer restores the energy to the source. As a result, the residual flux decreases and the core is demagnetized. This is demonstrated in Fig. 16 where the linkage flux of the two transformers is compared with transient simulations.

2) Design Considerations for Mitigation of the Phase-Hop Currents: The second set of experiments is carried out on the annealed, 2 mil, and the unannealed core transformers that are designed for different flux densities (1.5, 1.25, 1.12, 1, 0.87, and 0.75 T). The results are presented in Table VII. The annealed core transformers draw a considerably higher phase-hop currents than the 2 mil and unannealed core at the rated 1.5

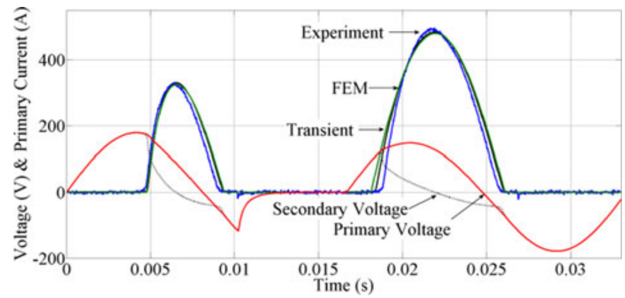

Fig. 14. Comparison of simulations and experiments for the phase-hop condition for T1 (nongapped); voltage and current from experiments and simulated current with FEM and transient simulations. The first peak of the current is the zero crossing inrush current and the second peak is the phase-hop current.

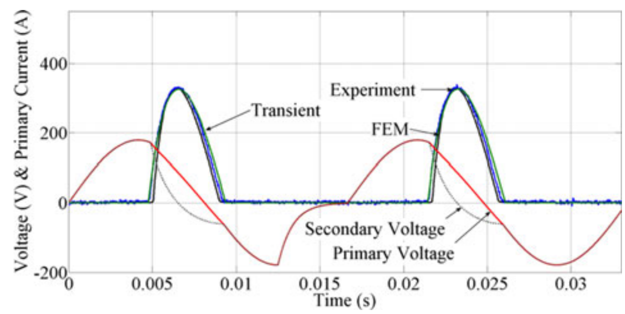

Fig. 15. Comparison of model and experiment for the phase-hop condition for T2 (gapped); voltage and current from experiments and simulated with FEM and transient simulations. The first peak of the current is the zero crossing inrush current and the second peak is the phase-hop condition.

T. This is so because the residual fluxes of these transformers are smaller than in the annealed core ones (see Figs. 6 and 10). Overall, the phase-hop current of the annealed core transformers is larger than that of the 2 mil and unannealed core transformers.

Assuming that transformers are designed with the same flux densities, the gapped transformer performs better to reduce the phase-hop currents. The active power losses are the same for the unannealed and the gap transformers. However, the gapped transformer draws larger magnetizing current which is the indication of a higher reactive power required by this transformer. Assuming the same mitigation factor, the transformer designed with unannealed core draws less reactive and active power; however, it is larger and heavier because it should be designed for lower flux density. For example to reduce the phase-hop about 75%, the unannealed transformer consumes almost 50% less reactive and 30% less active power, but the transformer needs to be designed at about 10% lower flux density when compared to the gapped transformer, which increases the size and weight (see Table VII).

The results presented in Table VII indicate that gapped transformers are more efficient reducing inrush and phase-hop currents, but with higher capital cost (CAPEX) and operation costs (OPEX). However, for a space or weight restricted application, where the acquisition cost is a less important factor than size and weight, gapped transformers are superior.

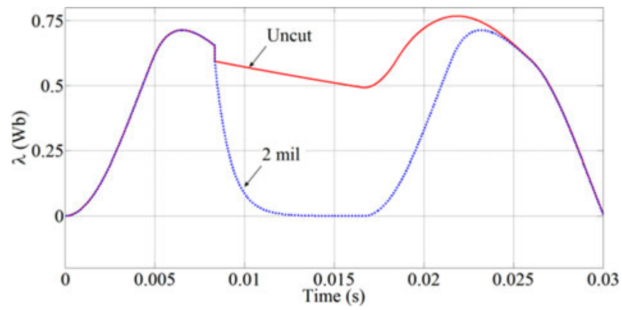

Fig. 16. Linkage flux of the two transformers obtained by transient simulations.

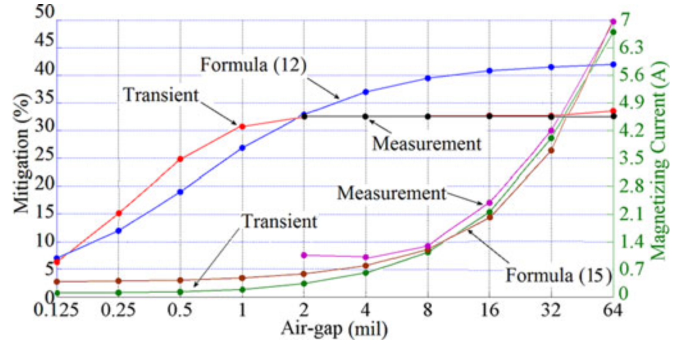

Fig. 17. Parametric study of (12) and (15) in terms of air-gap distance.

TABLE VII
EXPERIMENTAL RESULTS OF ANNEALED, UNANNEALED, AND 2-MIL GAPPED TRANSFORMERS

	Flux Density [T]	1.5	1.25	1.12	1	0.87	0.75
Inrush [A]	Annealed	330	94	58	1.5	0.38	0.1
	2-mil gap	330	105	47	3.2	1.3	1.2
	Unannealed	310	100	55	6.7	4.8	2.7
Phase-hop [A]	Annealed	490	255	210	175	125	50
	2-mil gap	330	112	53	3.6	1.4	1.2
	Unannealed	366	164	116	74	30	8
I_{mag} [mA]	Annealed	70	45	38	33	29	26
	2-mil gap	900	770	740	680	610	570
	Unannealed	1770	720	390	190	100	70
P_0 [W]	Annealed	6	4	3	2	2	1
	2-mil gap	15	7	5	4	3	2
	Unannealed	15	7	5	4	3	2

Phase-hop current, magnetizing current, and no-load power for different flux densities.

It should be noted that both of the mechanical procedures to anneal and create a gap (cut and reunite), increases the acquisition cost. The cut core transformers purchased for this study cost about twice than the uncut transformers. Generally, the acquisition cost or the total ownership cost of a product dictates the technology that can be implemented for a special problem. The selection of a solution shall be made with a tradeoff between the total cost, required operation characteristics, and the mitigation capability. For this purpose, transformer manufacturers need to understand the target market. There are many different applications for toroidal transformers in a wide variety of industries. Users have different requirements, constraints, preferences, and specifications.

3) Validation of (12) and (15): The analytical formulae (12) and (15) derived above for the calculation of the optimum air-gap length and the calculation of magnetizing current, respectively, are validated with laboratory experiments and transient simulations next.

Some of the parameters are obtained from the open-circuit test of uncut transformer (T1). These are: $\lambda_{r1} = 0.54$, $\lambda_s = 0.59$, $Q_{\mathrm{OC}} = 7.33$ var. The mitigation factor is calculated by substitution of the parameters in (12) and varying the air-gap length. The calculated results are compared to measurements and transient simulations in Fig. 17. Note that, measurements results only include 2, 4, 8, 16, 32, and 64 mil gapped transformers. As one can observe, the mitigation factors computed by (12) are in agreement with measurements and simulations (the maximum difference is about 7% for large gaps). The corresponding magnetizing currents for all transformers are shown in Fig. 17 with the comparison of (15) and simulations (as reference, the rated current is 8.33 A). As one can observe, the magnetizing currents computed by (15) are in agreement with measurements and simulations as well.

Note that, measurements and simulation results show that the mitigation factor of a transformer does not change by increasing the length of the air-gap after some point (in this case, $g > 2$ mil). However, the magnetizing current increases with g. Therefore, the minimum air-gap that satisfies the design conditions should be used. We remark that gaps smaller than 2 mil are difficult to control during manufacturing.

4) Voltage Sags and Notching Examples: This section is dedicated to evaluate the effect of the solutions on the parallel switching. To create voltage sags and notching in the laboratory, the parallel MOSFETs of the switch need to be activated. First, the series switch closes. After 0.5 of a cycle, the parallel MOSFETs are closed. Then to clear the fault the parallel switches are opened.

The effect of the air-gap for parallel switching conditions is different when compared to the voltage interruption and UPS systems. Laboratory measurements show that even for the 64 mil transformer, the air-gap is not effective to reduce the phase-hop currents. Similar results were found from experiments with the unannealed transformer.

For phase-hop currents caused by parallel switching, the only effective solution is to reduce the operating flux density at the design stage.

VI. CONCLUSION

In this paper, the effect of air-gaps and low-permeability iron core materials on inrush currents has been investigated. The following conclusions are confirmed with numerous laboratory experiments, FEM calculations, and time domain simulations:

1) Air-gaps are capable of controlling the magnetizing curve of transformers. Formulae are provided in this paper to compute the required air-gap length for a given application.
2) Air-gaps are capable of demagnetizing the transformer core when it is disconnected from the source and open circuited.

3) This paper proves that the use of air gaps does not reduce the inrush currents when transformers are fully demagnetized.
4) The air gap produces a significant reduction on the inrush currents when the transformer has residual flux, e.g., in the phase-hop conditions. It reduces the level of the phase-hop currents to the magnitude of the common inrush currents when phase-hop currents are caused by interruption and malfunction of UPS systems.
5) Air-gaps are not efficient mitigating phase-hop currents caused by notching and voltage sag.
6) Inrush current can be mitigated to the transformer nominal current level with a carefully designed low permeability iron core transformer.
7) Low-permeability cores are effective mitigating the phase-hop current; however, this mitigation is not as effective as air-gap for transformers designed with the same flux density. For the same mitigation capability, low-permeability materials consume less active and reactive losses (lower OPEX) and are less expensive (CAPEX is about half).
8) For space or weight restricted applications where price is not as important, air-gaps are recommended. For other applications, low-permeability iron materials are superior for inrush and phase-hope current mitigation.

Because the occurrence of phase-hop currents is unpredictable, a transformer-based solution, e.g., air-gaps or low-permeability iron core material, is needed. With these methods, there is no need of additional control and monitoring devices. Therefore, the proposed transformer-based solutions are reliable, simple, and cost-effective ways to mitigate the phase-hop currents. To avoid excessive magnetizing currents caused by large air-gaps, the minimum gap length that can effectively mitigate the phase-hop currents is calculated with analytical formulae.

References

[1] L. F. Blume, G. Camilli, S. B. Farnham, and H. A. Peterson, “Transformer magnetizing inrush currents and influence on system operation,” *AIEE Trans. Power App. Syst.*, vol. 63, pp. 366–375, Jan. 1944.

[2] P. C. Y. Ling and A. Basak, “Investigation of magnetizing inrush current in a single-phase transformer,” *IEEE Trans. Magn.*, vol. 24, no. 6, pp. 3217–3222, Nov. 1988.

[3] A. Farazmand, F. de León, K. Zhang, and S. Jazebi, “Analysis, modeling and simulation of the phase-hop condition in transformers: The largest inrush currents,” *IEEE Trans. Power Del.*, vol. 29, no. 4, pp. 1918–1926, Aug. 2014.

[4] A. K. Al-Khalifah and E. F. El-Saadany, “Investigation of magnetizing inrush current in a single-phase transformer,” in *Proc. IEEE Large Eng. Syst. Conf. Power Eng.*, 2006, pp. 165–171.

[5] K. Billings and T. Morey, *Switch Mode Power Supply Handbook*. New York, NY, USA: McGraw Hill, 1989, pp. 1–6.

[6] J. H. Brunke and K. J. Frohlich, “Elimination of transformer inrush currents by controlled switching. I. Theoretical considerations,” *IEEE Trans. Power Del.*, vol. 16, no. 2, pp. 276–280, Apr. 2001.

[7] J. H. Brunke and K. J. Frohlich, “Elimination of transformer inrush currents by controlled switching. II. Application and performance considerations,” *IEEE Trans. Power Del.*, vol. 16, no. 2, pp. 281–285, Apr. 2001.

[8] N. Chiesa and H. K. Hoidalen, “Novel approach for reducing transformer inrush currents: Laboratory measurements, analytical interpretation and simulation studies,” *IEEE Trans. Power Del.*, vol. 25, no. 4, pp. 2609–2616, Oct. 2010.

[9] A. Reis, J. C. de Oliveira, R. Apolonio, and H. S. Bronzeado, “A controlled switching methodology for transformer inrush current elimination: Theory and experimental validation,” in *Proc. IEEE 11th Int. Conf. Electr. Power Quality Utilization*, 2011, pp. 1–6.

[10] B. Kovan, F. de León, D. Czarkowski, Z. Zabar, and L. Birenbaum, “Mitigation of inrush current in network transformers by reducing the residual flux with and ultra-low-frequency power source,” *IEEE Trans. Power Del.*, vol. 26, no. 3, pp. 1563–1570, Jul. 2011.

[11] Y. Cui, S. G. Abdulsalam, S. Chen, and W. Xu, “A sequential phase energization technique for transformer inrush current reduction - Part I: Simulation and experimental results,” *IEEE Trans. Power Del.*, vol. 20, no. 2, pp. 943–949, Apr. 2005.

[12] W. Xu, S. G. Abdulsalam, Y. Cui, and X. Liu, “A sequential phase energization technique for transformer inrush current reduction - Part II: Theoretical analysis and design guide,” *IEEE Trans. Power Del.*, vol. 20, no. 2, pp. 950–957, Apr. 2005.

[13] Y. H. Chen, C. Y. Lin, J. M. Chen, and P. T. Cheng, “An inrush mitigation technique of load transformers for the series voltage sag compensator,” *IEEE Trans. Power Electron.*, vol. 25, no. 8, pp. 2211–2221, Aug. 2010.

[14] P. T. Cheng, W. T. Chen, Y. H. Chen, C. L. Ni, and J. Lin, “A transformer inrush mitigation method for series voltage sag compensators,” *IEEE Trans. Power Electron.*, vol. 22, no. 5, pp. 1890–1899, Sep. 2007.

[15] M. T. Hagh and M. Abapour, “DC reactor type transformer inrush current limiter,” *IET Electr. Power App.*, vol. 1, no. 5, pp. 808–814, Sep. 2007.

[16] H. T. Tseng and J. F. Chen, “Voltage compensation-type inrush current limiter for reducing power transformer inrush current,” *IET Electr. Power App.*, vol. 6, no. 2, pp. 101–110, Feb. 2012.

[17] S. M. Madani, M. Rostami, G. B. Gharehpetian, and R. Hangmaram, “Improved bridge type inrush current limiter for primary grounded transformers,” *Electr. Power Syst. Res.*, vol. 95, pp. 1–8, Feb. 2013.

[18] S. M. Madani, M. Rostami, G. B. Gharehpetian, and R. Hangmaram, “Inrush current limiter based on three-phase diode bridge for Y-yg transformers,” *IET Electr. Power App.*, vol. 6, no. 6, pp. 345–352, Jul. 2012.

[19] V. Molcrette, J. Kotny, J. Swan, and J. Brudny, “Reduction of inrush current in a single-phase transformer using virtual air-gap technique,” *IEEE Trans. Magn.*, vol. 34, no. 4, pp. 1192–1194, Jul. 1998.

[20] S. Magdaleno and C. Pérez Rojas, “Control of the magnetizing characteristics of a toroidal core using virtual gap,” in *Proc. IEEE Electron., Robot. Autom. Mech. Conf.*, 2010, pp. 540–545.

[21] B. Gladstone, “Magnetic solution: Solving inrush current at the source,” *Power Electron. Tech.*, pp. 14–26, Apr. 2004.

[22] *IEEE Recommended Practice for Powering and Grounding Electronic Equipment*, IEEE Standard 1100-1999, Mar. 1999.

[23] *IEEE Recommended Practice for Monitoring Electric Power Quality*, IEEE Standard 1159-1995, Jun. 1995.

[24] *IEEE Recommended Practice and Requirements for Harmonic Control in Electrical Power Systems*, IEEE Standard 519-1992, Apr. 1993.

[25] *IEEE Standard Test Code for Dry-Type Distribution and Power Transformers, Recognized as an American National Standard (ANSI)*, IEEE Standard C57.12.91-1995, 1995.

[26] S. Jazebi, F. de León, A. Farazmand, and D. Deswal, “Dual reversible transformer model for the calculation of low-frequency transients,” *IEEE Trans. Power Del.*, vol. 28, no. 4, pp. 2509–2517, Oct. 2013.

[27] E. C. Cherry, “The duality between interlinked electric and magnetic circuits and the formation of transformer equivalent circuits,” *Proc. Phys. Soc.*, vol. (B) 62, pp. 101–111, Feb. 1949.

[28] J. Billan, “Coercimeter for non-destructive measurement of the coercivity of steel sheets,” *J. Phys. Colloques*, vol. 45, no. C1, pp. 965–968, Jan. 1984.

[29] F. de León, A. Farazmand, and P. Joseph, “Comparing T and Pi equivalent circuits for the calculation of transformer inrush currents,” *IEEE Trans. Power Del.*, vol. 27, no. 4, pp. 2390–2398, Oct. 2012.

[30] Y. Wang, S. G. Abdulsalam, and W. Xu, “Analytical formula to estimate the maximum inrush current,” *IEEE Trans. Power Del.*, vol. 23, no. 2, pp. 1266–1268, Apr. 2008.

[31] S. Jazebi, F. de León, and N. Wu, “Enhanced analytical method for the calculation of the maximum inrush currents of single-phase power transformers,” *IEEE Trans. Power Del.*, (DOI: 10.1109/TPWRD.2015.2443560). (Early Access).

[32] K. J. Overshott and M. H. Price, “The effect of annealing conditions on the power loss of amorphous ribbons,” *IEEE Trans. Magn.*, vol. 18, no. 6, pp. 1394–1396, Nov. 1982.

[33] F. de León, S. Jazebi, and A. Farazmand, “Accurate measurement of the air-core inductance of iron-core transformers with a non-ideal low power rectifier,” *IEEE Trans. Power Del.*, vol. 29, no. 1, pp. 294–296, Feb. 2014.

Rasim Dogan received the B.Sc. degree in electrical and electronics engineering from Gazi University, Ankara, Turkey, in 2008, the M.Sc. degree in electrical engineering from the NYU Polytechnic School of Engineering, Brooklyn, NY, USA, in 2012, and is currently working toward the Ph.D. degree in electrical engineering at the NYU Polytechnic School of Engineering.

His research interests include simulation and calculation of electromagnetic fields applied to transformers.

Saeed Jazebi (S'10–M'14) was born in Kerman, Iran. He received the B.Sc. degree in electrical engineering from Shahid Bahonar University, Kerman, in 2006, the M.Sc. degree in electrical engineering from the Amirkabir University of Technology, Tehran, Iran, in 2008, and the Ph.D. degree in electrical engineering from the NYU Polytechnic School of Engineering, Brooklyn, NY, USA, in 2014.

He is continuing his research as a Postdoctoral Fellow at the NYU Polytechnic School of Engineering. His fields of interest include electromagnetic design, modeling and simulation of electrical machines and power system components, power system protection, and power quality.

Francisco de León (S'86–M'92–SM'02–F'15) received the B.Sc. and the M.Sc. (Hons.) degrees in electrical engineering from the National Polytechnic Institute, Mexico City, Mexico, in 1983 and 1986, respectively, and the Ph.D. degree in electrical engineering from the University of Toronto, Toronto, ON, Canada, in 1992.

He has held several academic positions in Mexico and has worked for the Canadian electric industry. He is currently an Associate Professor at the Department of Electrical and Computer Engineering, New York University, New York, NY, USA. His research interests include the analysis of power phenomena under nonsinusoidal conditions, the transient and steady-state analyses of power systems, the thermal rating of cables and transformers, and the calculation of electromagnetic fields applied to machine design and modeling.

Dr. León is an Editor of the IEEE Transactions on Power Delivery and the IEEE Power Engineering Letters.